Available online at www.sciencedirect.com
ScienceDirect
Tetrahedron
Tetrahedron 63 (2007) 3538–3547

Triad base pairs containing fluorene unit for quencher-free SNP typing

Jin Ho Ryu,[a] Young Jun Seo,[a] Gil Tae Hwang,[a] Jin Yong Lee[b] and Byeang Hyean Kim[a,*]

[a]*National Research Laboratory, Department of Chemistry, BK School of Molecular Science, Pohang University of Science and Technology, Pohang 790-784, Republic of Korea*

[b]*Department of Chemistry, Sungkyunkwan University, Suwon 440-746, Republic of Korea*

Received 10 April 2006; revised 18 October 2006; accepted 18 October 2006
Available online 3 February 2007

Abstract—We designed an A-selective fluorescent DNA probe, $\mathbf{U^{FL}}$, which bears a 2-ethynylfluorene moiety covalently attached to the base dU, and incorporated it into a central position in the hairpin loop. We describe photophysical studies of triad base pairs containing an $\mathbf{U^{FL}}$ DNA probe and their application to single-nucleotide polymorphism (SNP) typing using novel quencher-free molecular beacons (MBs). The drastic changes in the fluorescence properties that arise upon changing the nature of the complementary base and FBs suggest that these triad base pairs are the key elements for quencher-free SNP typing.

1. Introduction

In the post-genome era, one rapidly growing area of research is that directed at comprehensively investigating the genomic information provided by single-nucleotide polymorphisms (SNPs).[1] SNPs change both the structures and functions of their encoded proteins and, thus, they are related directly to the physiological features of living systems. These nucleotide variations within the genome are in some cases linked to the variable responses toward drugs in different patients.[2] Reliable methods for the rapid screening of SNPs are highly desired for studying and identifying disease-causing genes. Thus, the high-throughput, economical, and precise detection of SNPs is a key issue in the modern fields of chemical biology, biotechnology, medicine, and pharmacogenomics.[3] Currently, there are several methods that have been developed for SNP typing; some of them are already commercially available. These methods include the use of (a) probe–target hybridization,[4] (b) enzymatic reactions (such as cleavage,[5] digestion,[6] minisequencing,[7] and primer elongation[8]), (c) DNA chips,[9] and (d) nanoparticle-labeled oligonucleotides.[10] In addition to these methods, we are interested in using chemically modified fluorescence probes. Fluorescent-labeled DNA probes are powerful gene-targeting agents for simplifying DNA probe assays; upon hybridization with their target sequences, the fluorescence undergoes a drastic change in either its intensity or emissive color. As a result, the bases on the complementary strands can be determined fluorometrically without the need for any separation or washing procedures.[11] Two representative approaches have been developed in the search for fluorescent probes for use in SNP typing. One improved version of a promising gene detection tool is the so-called 'molecular beacons' (MBs), which are a newly developed class of DNA probes that operate through fluorescence resonance energy transfer (FRET).[4] Traditional MBs are doubly end-labeled oligonucleotides that exist in solution as stable stem-loop structures in which the fluorescence of a reporter dye attached to the 5′ end is quenched through energy transfer to a proximate quencher attached to the 3′ end. In the presence of a complementary nucleic acid, the stem opens and this event is signaled by a loss of quenching and an increase in fluorescence. A number of MBs possess significant advantages over conventional DNA probes; these systems include (1) metal-containing MBs,[12] (2) MBs possessing two fluorophores,[13] (3) linear MBs possessing a fluorophore and a quencher,[14] (4) HyBeacons and dual-labeled probes,[15] (5) catalytic MBs,[16] and (6) excimer–monomer switching MBs.[17] The other successful method for the selective detection of SNPs involves the modification of nucleotide bases. Fluorescent nucleotide base analogues have been investigated as probes for reporting the dynamics of DNA.[18] Because the fluorescence is sensitive to the microenvironment surrounding the fluorescent chromophore, these nucleotide base analogues have also been utilized to report the degree of hybridization. A series of novel modified nucleotide bases are known to emit fluorescence upon their hybridizations to a specific nucleotide base.[19] Such modifications are particularly valuable because the natural bases

* Corresponding author. Tel.: +82 54 279 2115; fax: +82 54 279 3399; e-mail: bhkim@postech.ac.kr

0040–4020/$ - see front matter © 2007 Elsevier Ltd. All rights reserved.
doi:10.1016/j.tet.2006.10.091

are practically non-emissive[20] and end labeling with fluorescent tags is not necessarily a sensitive approach to monitoring remote binding events. No universal solutions exist, however, and additional modifications must be developed and evaluated empirically.

Recently, we reported a new type of MB—a quencher-free MB for SNP typing—that consists of only a single fluorophore in the hairpin loop, i.e., the system operates without a quencher.[21] We assumed that if the fluorene moiety is attached covalently to a uracil moiety at the C-5 position through a rigid ethynyl linker, the fluorophore would protrude from the resulting DNA helix—upon its base pairing with its matched strand—and undergo weak interactions with its neighboring nucleobases.[22] In such a case, the fluorene-labeled DNA probe should exhibit a strong A-selective fluorescence. In contrast, when the fluorene unit is intercalated (located) within a DNA duplex in the absence of base pairing (mismatched duplex), the $\mathbf{U^{FL}}$ unit would exhibit quenched fluorescence as a result of photoinduced charge transfer that originates from interactions with its neighboring nucleobases. Moreover, the fluorescence of $\mathbf{U^{FL}}$ displays a strong dependence on the nature of its flanking bases (FBs), which affect the electronic and conformational microenvironment of the triad base pairs. In this paper, we report the design and photophysical properties of triad base pairs containing $\mathbf{U^{FL}}$ moieties and their application to the formation of quencher-free MBs.

2. Results and discussion

2.1. Synthesis of fluorene-labeled modified oligonucleotides

The oligonucleotide model system was designed as a new type of MB consisting of a six-base-pair stem and a seven-base loop sequence containing a fluorene-labeled deoxyuridine core ($\mathbf{U^{FL}}$; Fig. 1).[21,23] We synthesized $\mathbf{U^{FL}}$ from the corresponding 5-iodo-2′-deoxyuridine[24]and 2-ethynylfluorene[25] through a Pd-catalyzed Sonogashira coupling,[26] and then converted it into the corresponding phosphoramidite building block for ODN synthesis.[27] The acetylene bridge of this structure provides the necessary structural rigidity to separate the fluorene group from the base stack, in which strong electronic coupling occurs between the fluorene and uridine moieties.[28] Moreover, we expected that the Watson–Crick base pairing properties of the dU should remain unchanged upon attaching the 2-ethynylfluorene moiety and that the introduction of $\mathbf{U^{FL}}$ should not perturb the formation of nucleic acid complexes because the rigid linker at the 5-position of $\mathbf{U^{FL}}$ directs the fluorene unit into the major groove of the duplex.[22]

Table 1. Photophysical properties of the fluorene-labeled ODNs 5′d-TTCTGA CTX$\mathbf{U^{FL}}$YTT TCAGAA

Sequence	X/Y[a]	T_m/°C[b]	λ_{max}/nm[c]	λ_{em}/nm[d]	FIR[e]
ODN1($\mathbf{U^{FL}}$)	T/T	51	319	429	1.01
ODN2($\mathbf{U^{FL}}$)	C/C	48	332	429	1.00
ODN3($\mathbf{U^{FL}}$)	A/A	45	331	431	0.93
ODN4($\mathbf{U^{FL}}$)	G/G	56	331	441	0.24
ODN5($\mathbf{U^{FL}}$)	C/T	48	331	431	1.09
ODN6($\mathbf{U^{FL}}$)	T/C	56	320	431	1.11
ODN7($\mathbf{U^{FL}}$)	A/G	56	332	433	0.67
ODN8($\mathbf{U^{FL}}$)	G/A	54	331	433	0.29

[a] Flanking bases.
[b] Melting temperature.
[c] Maximum absorption wavelength.
[d] Emission wavelength, excited at 340 nm.
[e] Relative fluorescence intensity ratio compared to that of ODN2($\mathbf{U^{FL}}$). All samples were prepared using 10 mM Tris–HCl buffer (100 mM NaCl; 20 mM $MgCl_2$; pH 7.2).

We incorporated this $\mathbf{U^{FL}}$ unit into the central positions of eight oligodeoxyribonucleotides [from ODN1($\mathbf{U^{FL}}$) to ODN8($\mathbf{U^{FL}}$)] through the use of standard protocols in automated DNA synthesis (Table 1). To investigate the effect of the FBs on the fluorescence properties, we modified the ODNs primarily at the bases flanking the $\mathbf{U^{FL}}$ unit. It has been reported that the fluorescence properties of DNA are strongly dependent on the electron injection and transfer properties of the FBs. Among the DNA bases, those of thymine (T) and cytosine (C) can be reduced most easily.[28,29] On the other hand, guanine (G) has the lowest oxidation potential such that it can photoinitiate oxidative hole-injection/transfer.[30] After the synthesis, we purified the ODN($\mathbf{U^{FL}}$) derivatives using semi-preparative HPLC and identified them through MALDI-TOF mass spectrometry.

2.2. Photophysical properties of the fluorene-labeled hairpin oligonucleotides

Before investigating the photophysical properties of the fluorene-unit-containing hairpin ODNs, we measured the absorption and fluorescence spectra of the nucleoside $\mathbf{U^{FL}}$ in chloroform at a concentration of 1.0×10^{-5} M. The absorption maximum (λ_{max}) of $\mathbf{U^{FL}}$ appears at 325 nm, as is characteristic of fluorene chromophores. We observed a strong fluorescence at 405 nm upon excitation at 340 nm (quantum yield: Φ_F=0.139). Although the fluorescence of previously described similarly modified nucleosides with pyrene

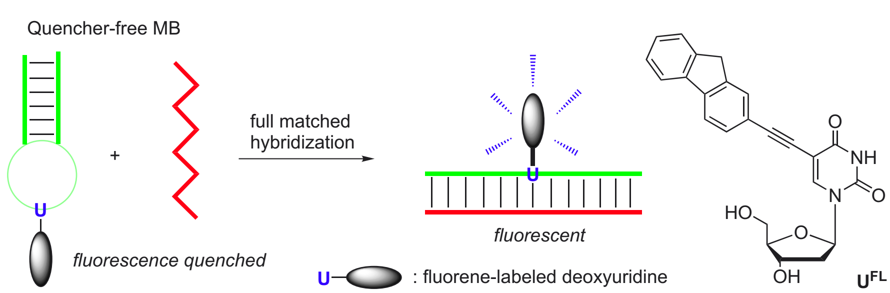

Figure 1. Schematic illustration of quencher-free MBs DNA sensor for SNPs typing and a fluorene unit $\mathbf{U^{FL}}$.

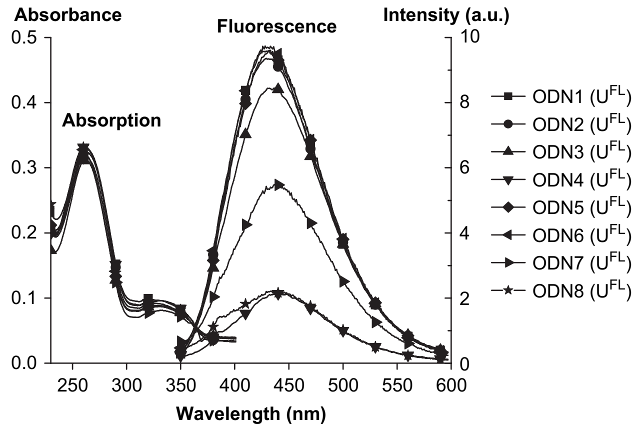

Figure 2. Absorption and fluorescence spectra of the single-stranded oligonucleotides ODN($\mathbf{U^{FL}}$) (1.5 μM) recorded in 10 mM Tris–HCl buffer (pH 7.2, 100 mM NaCl, 20 mM $MgCl_2$) at 25 °C. Excitation wavelength: 340 nm.

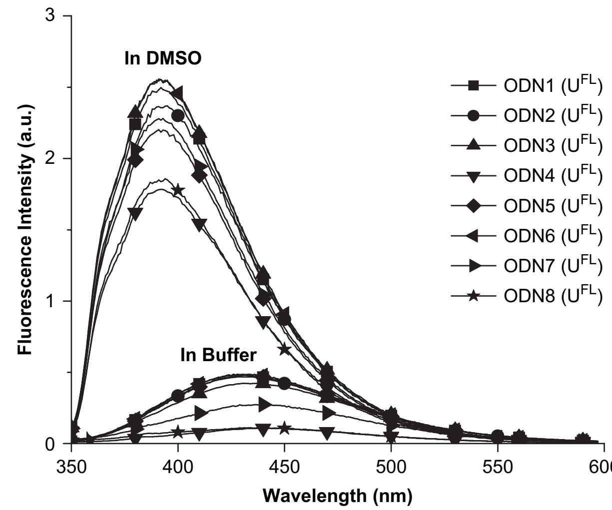

Figure 3. Fluorescence spectra of the single-stranded oligonucleotides ODN($\mathbf{U^{FL}}$) (1.5 μM) with comparing in buffer with in DMSO.

fluorophores is strongly dependent on the solvent polarity, $\mathbf{U^{FL}}$ displays only a slight variation in its fluorescence properties when dissolved in a more-polar solvent (in methanol: λ_{em}=407 nm; Φ_F=0.133).[28,31] We measured the absorption spectra of 1.5 μM solutions of the hairpin ODNs($\mathbf{U^{FL}}$) in Tris–HCl buffer (pH 7.2) containing 100 mM NaCl and 20 mM $MgCl_2$ (Fig. 2; Table 1). The spectra exhibit similar shapes and have absorption maxima (ca. 331 nm), except for those of ODN1($\mathbf{U^{FL}}$) and ODN6($\mathbf{U^{FL}}$) (ca. 320 nm), which possess a 5′-directed T-FB. Each absorption spectrum displays a broad absorbance near the fluorene region, despite the small variations in the absorption maxima, which suggests that the fluorene-labeled ODNs have similar absorption and ground state energies, i.e., they are independent on the nature of the FBs.

We recorded the fluorescence spectra of the hairpins ODN($\mathbf{U^{FL}}$) in the same buffer at an excitation wavelength of 340 nm to determine whether the FBs have any effect on the fluorescence levels in the hairpins. Indeed, we found that there was little difference between the fluorescence intensities, except for those of systems containing G moieties as FBs. Because G has the lowest oxidation potential of the nucleobases, it serves as a fluorescence quencher through electron transfer.[30] We have found that the quenching caused by G-FBs, the so-called 'G effect,' was highest in ODN4($\mathbf{U^{FL}}$), in which two G-FBs are present, and the 5′-direction is more affected than the 3′-direction by G [cf. ODN7($\mathbf{U^{FL}}$) and ODN8($\mathbf{U^{FL}}$)].

We also recorded the fluorescence spectra of hairpin ODNs (Fig. 3) at the same concentration in DMSO, which is a solvent that is known to disrupt the secondary structure of nucleic acids by interfering with the stacking interactions.[32] Remarkably, the fluorescence spectra of all of these hairpin ODNs in DMSO exhibit significant fluorescence enhancements and the abatement of the severe red-shifting of their emissions. These findings support the notion that disrupting the secondary structures of the hairpins no longer allows the electronic interactions to mediate fluorescence quenching. The G effect still exists in DMSO, but the relative effects were weaker than those we observed in the spectra recorded in buffer. Thus, the photophysical properties exhibited in the hairpin state are a consequence of the hairpins ODN($\mathbf{U^{FL}}$) having similar ground state energies. In addition, the influence that the FBs have on fluorescence in the hairpin is negligible, except for that of the G effect.

2.3. Photophysical properties of the fluorene-labeled DNA duplexes

For A-selective fluorescence emission of $\mathbf{U^{FL}}$ to occur it is necessary that the fluorene chromophore protrude from the DNA duplex when $\mathbf{U^{FL}}$/A base pairing occurs upon hybridization. Moreover, the incorporation of the moiety $\mathbf{U^{FL}}$ should not perturb the thermal stability or conformation of the DNA strand. To determine the manner through which hybridization occurs, initially we obtained the melting temperatures (T_m) and CD spectra of the double-stranded DNA (dsDNA) duplexes that were formed upon hybridization of the ODN($\mathbf{U^{FL}}$) strands with their corresponding complementary ODN(**A**) strands ([ODNs($\mathbf{U^{FL}}$)/ODNs(**A**)]) (Table 2; Fig. 4).

Table 2. Photophysical properties of the fluorene-labeled ODN($\mathbf{U^{FL}}$) duplexes (ODNs($\mathbf{U^{FL}}$): 5′d-TTCTGA CTX$\mathbf{U^{FL}}$YTT TCAGAA; ODNs(**A**): 3′d-AAGACT GAX′AY′AA AGTCTT[a])

Sequences	X/Y[b]	T_m/°C[c]	λ_{max}/nm[d]	λ_{em}/nm[e]	FCH[f]	FER[g]
ODN1($\mathbf{U^{FL}}$)/ODN1(**A**)	T/T	56	334	422	5.06	39.8
ODN2($\mathbf{U^{FL}}$)/ODN2(**A**)	C/C	58	333	424	2.20	18.9
ODN3($\mathbf{U^{FL}}$)/ODN3(**A**)	A/A	53	334	429	2.37	20.8
ODN4($\mathbf{U^{FL}}$)/ODN4(**A**)	G/G	58	334	446	0.41	1.00
ODN5($\mathbf{U^{FL}}$)/ODN5(**A**)	C/T	57	333	426	1.66	17.6
ODN6($\mathbf{U^{FL}}$)/ODN6(**A**)	T/C	56	332	426	2.82	32.0
ODN7($\mathbf{U^{FL}}$)/ODN7(**A**)	A/G	55	332	433	1.06	6.54
ODN8($\mathbf{U^{FL}}$)/ODN8(**A**)	G/A	56	334	449	0.50	1.34

[a] ODNs(**A**) are complementary to the corresponding fluorene-labeled ODNs($\mathbf{U^{FL}}$). X′ and Y′ are complementary bases for X and Y, respectively.
[b] Flanking bases.
[c] Melting temperature.
[d] Maximum absorption wavelength.
[e] Emission wavelength, excited at 340 nm.
[f] Ratio of relative change in fluorescence upon hybridization compared to nonhybridized hairpin.
[g] Relative fluorescence enhancement ratio. All experiments were conducted in 10 mM Tris–HCl buffer (pH 7.2, 100 mM NaCl, 20 mM $MgCl_2$).

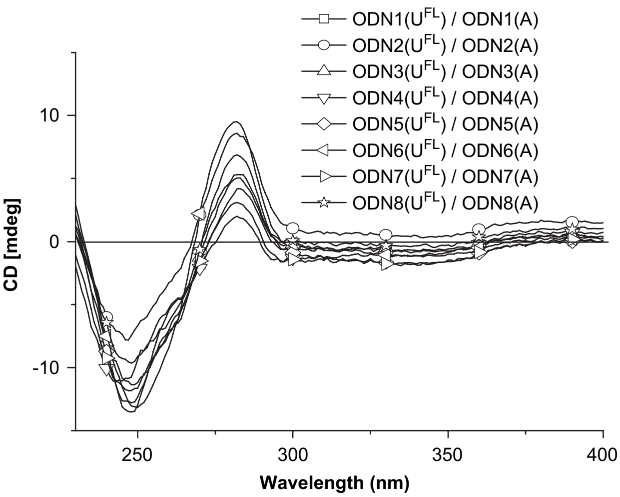

Figure 4. CD spectra of DNA duplexes [ODNs($\mathbf{U^{FL}}$)/ODNs(**A**)] (3.0 μM) in 10 mM Tris–HCl buffer (pH 7.2, 100 mM NaCl, 20 mM $MgCl_2$).

We observed that the T_m values of dsDNA systems having two G–C flanking base pairs [ODN2($\mathbf{U^{FL}}$)/ODN2(**A**), ODN4($\mathbf{U^{FL}}$)/ODN4(**A**)] are 2–5 degrees higher than those possessing T–A flanking base pairs [ODN1($\mathbf{U^{FL}}$)/ODN1(**A**), ODN3($\mathbf{U^{FL}}$)/ODN3(**A**)].[33] This general property provides evidence that the $\mathbf{U^{FL}}$ moiety does not interfere with the thermal stability of the triad base pairs. The CD spectra of all of the duplexes display overall B-DNA conformations. In conclusion, we believe that $\mathbf{U^{FL}}$ participates selectively in a base pair with A and maintains the normal shape of the resulting DNA duplex; further details are provided in later sections.

We measured the fluorescence spectra of the dsDNA [ODNs($\mathbf{U^{FL}}$)/ODNs(**A**)] at a concentration of 1.5 μM in the same aqueous buffer (Fig. 5; Table 2). The absorption spectra have similar shapes and absorption maxima (λ_{max}: 332–334 nm), which suggest that the ground state energies in the overall dsDNA duplexes are very similar.

The fluorescence excitation spectra of the hairpins and their matched duplexes bearing homogeneous FBs each exhibit a strong emission peak at 430 nm, except for those possessing a G moiety as FB.

The intensity of the peak that arises is strongly dependent on the nature of the FBs. This finding suggests that the conformation of the triad base pairs in each duplex is responsible for the differences in fluorescence, i.e., they are affected to a remarkable degree by the nature of the FBs. The fluorescence emission spectra of the matched duplexes display strong enhancements in fluorescence upon excitation at 340 nm, except for those possessing G moieties as FBs. The relative quantum yields decrease with respect to the nature of the FBs in the following order: T>C≈A>G. In addition, we also observed that the T-FB and G effects are more pronounced in the 5′-direction than they are in the 3′-direction.[28,34] Moreover, we could readily determine the influence on the steady state fluorescence upon hybridization, which is a measure of the degree of freedom of the conformation of $\mathbf{U^{FL}}$, through variable-temperature fluorescence spectroscopy (Fig. 6). As the temperature increased,

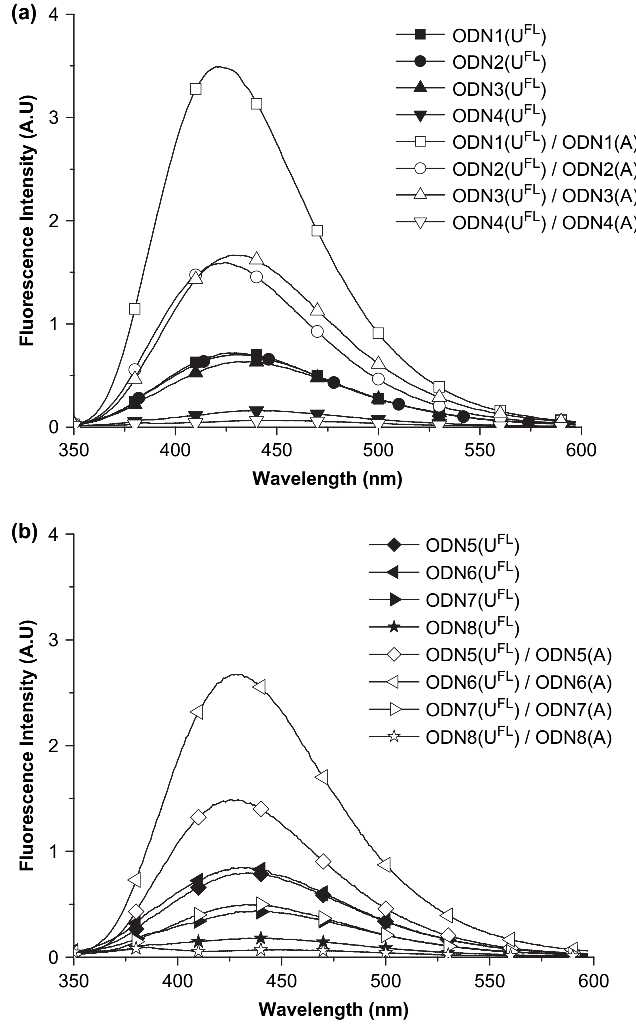

Figure 5. Fluorescence spectra of the double-stranded oligonucleotides ODNs($\mathbf{U^{FL}}$)/ODNs(**A**). (a) Fluorescence spectra of ODN1($\mathbf{U^{FL}}$)–ODN4($\mathbf{U^{FL}}$) having homogeneous FBs. (b) Fluorescence spectra of ODN5($\mathbf{U^{FL}}$)–ODN8($\mathbf{U^{FL}}$) having heterogeneous FBs. All spectra were recorded using 1.5 μM solutions of the samples in 10 mM Tris–HCl buffer (pH 7.2, 100 mM NaCl, 20 mM $MgCl_2$). Excitation wavelength: 340 nm.

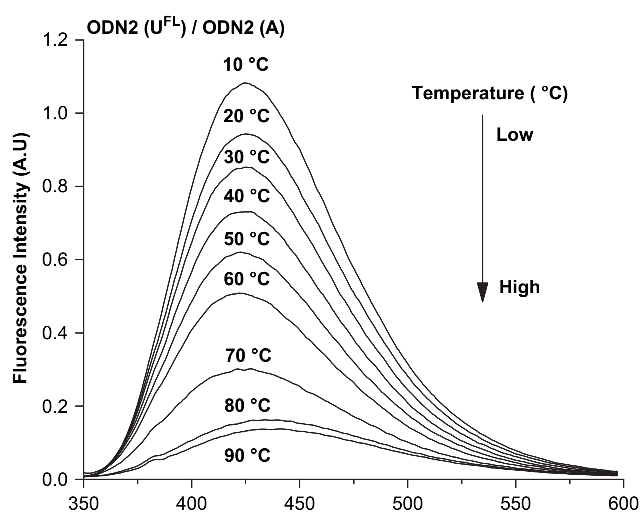

Figure 6. Variable-temperature fluorescence spectra of ODN2($\mathbf{U^{FL}}$)/ODN2(**A**) (1.5 μM) in 10 mM Tris–HCl buffer (pH 7.2, 100 mM NaCl, 20 mM $MgCl_2$). Excitation wavelength: 340 nm.

the fluorescence intensity of the excited state decreased because of disruption of the $\mathbf{U^{FL}}$/A base pair.

In summary, the relative fluorescence intensities exhibited upon hybridization are affected by the nature of the FBs and depend upon the microenvironments experienced by the $\mathbf{U^{FL}}$ moieties. This finding suggests the importance of the rigid conformations of the triad base pairs.

2.4. Quencher-free SNP typing

If $\mathbf{U^{FL}}$ displays a highly A-selective fluorescence emission then the fluorescence change derived from the nature of a complementary base would be extremely useful for this system's application to quencher-free SNP typing. To confirm their potential as SNP probes, we determined the discriminations toward single-nucleotide modifications displayed by the fluorescent ODNs having different FBs [ODN1($\mathbf{U^{FL}}$)–ODN4($\mathbf{U^{FL}}$); Fig. 7]. Upon hybridization with their target and mismatched sequences, the ODN1($\mathbf{U^{FL}}$) and ODN2($\mathbf{U^{FL}}$) systems, which possess only pyrimidine FBs, exhibited A-selective fluorescence at 430 nm, as indicated in Figure 7. In contrast, the ODNs($\mathbf{U^{FL}}$) bearing purine FBs display no discrimination activity toward any nucleobases. In particular, the ODN2($\mathbf{U^{FL}}$) probe, which has C moieties as FBs, acts as a highly A-allele-selective fluorescent 'on/off' switch for the detection of SNPs. Upon hybridization with a perfectly matched target, i.e., one that produces a $\mathbf{U^{FL}}$/A base pair, the intensity of the fluorescence at 425 nm upon excitation at 340 nm displayed a 2.2-fold increase. In contrast, the formation of $\mathbf{U^{FL}}$/N′ mismatched base pairs resulted in 0.18 (N′=T), 0.15 (N′=C), and 0.12-fold (N′=G) decreases in the fluorescence intensity. Therefore, the total discrimination factors are 12.2 (T), 14.7 (C), and 18.3 (G) for the recognition of a single base mismatch.

2.5. Using of abasic site containing DNA strands

We examined abasic site (ϕ) effect to clarify the triad base pair system by incorporating the tetrahydrofuranyl residues into the ODNs.[35] Table 3 lists the four ODNs(ϕ) that we synthesized: ODN1(ϕ) possessing ϕ-FBs and the fluorescent

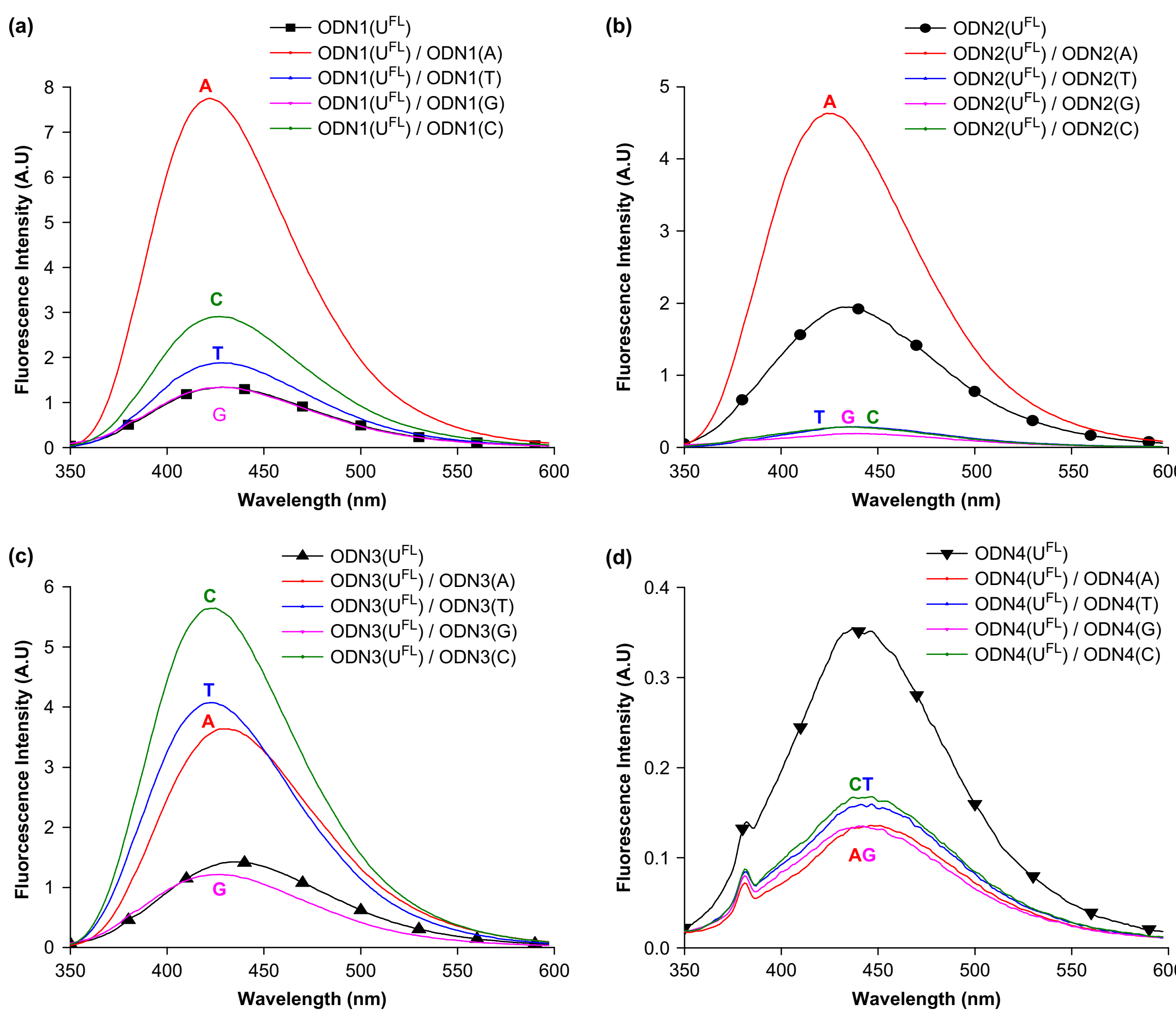

Figure 7. Fluorescence spectra of ODNs($\mathbf{U^{FL}}$)/ODNs(N) systems (5′d-TTCTGA CTX$\mathbf{U^{FL}}$YTT TCAGAA/3′d-AAGACT GAX′NY′AA AGTCTT; X, Y=flanking bases; X′, Y′=complementary bases for X, Y; N=A, T, G, C). (a) ODN1($\mathbf{U^{FL}}$)/ODN1(N), T-FB; (b) ODN2($\mathbf{U^{FL}}$)/ODN2(N), C-FB; (c) ODN3($\mathbf{U^{FL}}$)/ODN3(N), A-FB; (d) ODN4($\mathbf{U^{FL}}$)/ODN4(N), G-FB. All samples were prepared as 1.5 μM solutions in 10 mM Tris–HCl buffer (pH 7.2; 100 mM NaCl, 20 mM $MgCl_2$). Excitation wavelength: 340 nm.

Table 3. Abasic site (ϕ)-containing oligodeoxynucleotides

ODNs	Sequence/conditions
ODN1(ϕ)	5′ TTCTGA AA ϕ **U**$^{\mathbf{FL}}$ϕ AG TCAGAA/ abasic flanking units
ODN2(ϕ)	5′ TTCTGA AAG ϕ GAG TCAGAA/ abasic complementary unit
ODN3(ϕ)	5′ TTCTGA AA ϕ A ϕ AG TCAGAA
ODN4(ϕ)	5′ TTCTGA AA ϕ C ϕ AG TCAGAA/ imperfect match, abasic flanking units

U$^{\mathbf{FL}}$ moiety; ODN2(ϕ), a complementary strand possessing a ϕ unit; ODN3(ϕ) and ODN4(ϕ) which possess ϕ-FBs and A and C moieties, respectively.

With respect to both the fluorescence intensity and the emissive color, the fluorescence emission spectrum of ODN1(ϕ) is very similar to those of all the hairpins ODNs(**U**$^{\mathbf{FL}}$), except for G effect (Fig. 8, Table 4). This finding indicates that the FBs have a minimal effect in the hairpin state.

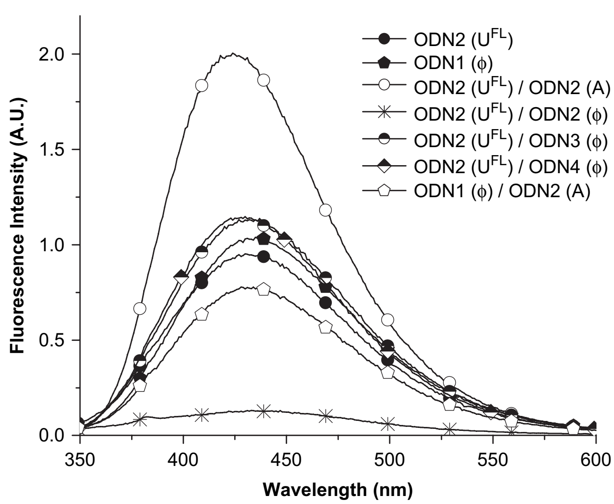

Figure 8. Fluorescence spectra of the abasic site (**ϕ**)-containing DNA duplexes, compared with those using the ODN2(**U**$^{\mathbf{FL}}$) system (1.5 μM), recorded in 10 mM Tris–HCl buffer (pH 7.2; 100 mM NaCl, 20 mM $MgCl_2$).

Table 4. Photophysical properties of the abasic site (ϕ)-containing DNA duplexes relative to those of the ODN2(**U**$^{\mathbf{FL}}$) system

Sequences	T_m/°C[a]	λ_{em}/nm[b]	FIR[c]
ODN1(ϕ)	45	435	1.06
ODN2(**U**$^{\mathbf{FL}}$)/ODN2(ϕ)	55	433	0.16
ODN2(**U**$^{\mathbf{FL}}$)/ODN3(ϕ)	46	432	1.17
ODN2(**U**$^{\mathbf{FL}}$)/ODN4(ϕ)	46	430	1.16
ODN2(**T**)[d]/ODN(ϕ)	43	none	none

All experiments were conducted in 10 mM Tris–HCl buffer (pH 7.2; 100 mM NaCl, 20 mM $MgCl_2$).
[a] Melting temperature.
[b] Emission wavelength, excited at 340 nm.
[c] Ratio of fluorescence intensities, relative to that of using ODN2(**U**$^{\mathbf{FL}}$).
[d] ODN(**T**)=5′d-TTCTGA CTC**T**CTT TCAGAA, a hairpin having the same, but unmodified, sequence as ODN2(**U**$^{\mathbf{FL}}$).

Thus, the fluorescence intensity of our quencher-free MB is diminished by electronic interactions induced in the randomly folded loop structure, not by the nature of the FBs. Next, we performed experiments to understand why fluorescence quenching occurred in the mismatched cases. We believe that the decreased fluorescence originates from flipping of the **U**$^{\mathbf{FL}}$ moiety near the core of the helix when base paring is absent. Upon incorporation of the abasic site into the complementary opposite strand, the emission intensity decreased dramatically upon the hybridization of ODN2(ϕ) with ODN2(**U**$^{\mathbf{FL}}$). In addition, this system displayed an enhanced thermal stability (ΔT_m=12 °C) when compared with the hybridization of ODN2(ϕ) with ODN(T), which is a hairpin having the same, but unmodified, sequence as ODN2(**U**$^{\mathbf{FL}}$). The fluorescence quenching phenomena and the increasing T_m of ODN2(ϕ) with ODN2(**U**$^{\mathbf{FL}}$) strongly suggest that the mechanism of quenching may be originated on the significant stacking interaction that occurs with the two complementary G-FBs upon flipping of the **U**$^{\mathbf{FL}}$ moiety.[35]

Moreover, the imperfect FB pairings did not lead to any fluorescence enhancements upon the hybridization of ODN2(**U**$^{\mathbf{FL}}$) with either its matched or mismatched strands [i.e., ODN2(**U**$^{\mathbf{FL}}$)/ODN3(ϕ) or ODN2(**U**$^{\mathbf{FL}}$)/ODN4(ϕ)]. In addition, it is an attractive feature that we may also use the **U**$^{\mathbf{FL}}$-containing systems for the recognition of the abasic nucleoside, i.e., providing an expanded set of SNPs. Naturally occurring abasic sites are a common form of DNA damage; they are formed upon alkylation of DNA bases followed by hydrolysis of the glycosidic bond, base excision repair, and spontaneous hydrolytic loss of purine units.[36]

In contrast to several known ligand-based methods for the detection of SNPs,[37] our quencher-free systems allow the simultaneous detection of abasic sites and target sequences including single-nucleotide modifications.

2.6. Computational analysis

We performed quantum chemical calculations to pinpoint the experimental fluorescence behavior of the hairpins and their matched and single-base-mismatched duplexes. For typical MBs, the change in fluorescence is believed to occur through electron transfer to a quencher. In our quencher-free MBs, we assume that the fluorescence behavior is controlled through electron transfer to neighboring groups and/or intermolecular interactions between fluorene and neighboring groups. We believe that the fluorescence behavior of the fluorene linked to the central base through an acetylene linker is influenced most strongly by the nearest neighboring base units, and only negligibly by the second-nearest (or further) base units. Most calculations performed on ODNs to date have been performed using force field calculations to obtain structural information;[38] because of computational limitations, ab initio calculations are mostly used when focusing on the electronic structures and properties of single base pairs.[39] Thus, we choose to model a simple ODN system, denoted as C**U**$^{\mathbf{FL}}$C [cf. the composition of ODN2(**U**$^{\mathbf{FL}}$)], that is composed of two cytidine (C) units and a central uridine (U) unit bearing the fluorene fluorophore.

We focused on the C**U**$^{\mathbf{FL}}$C system in an effort to understand the experimental fluorescence spectra, believing that the results for other systems would be comparable. Our molecular systems are very large—they are duplexes containing three base pairs—and so we first performed semi-empirical

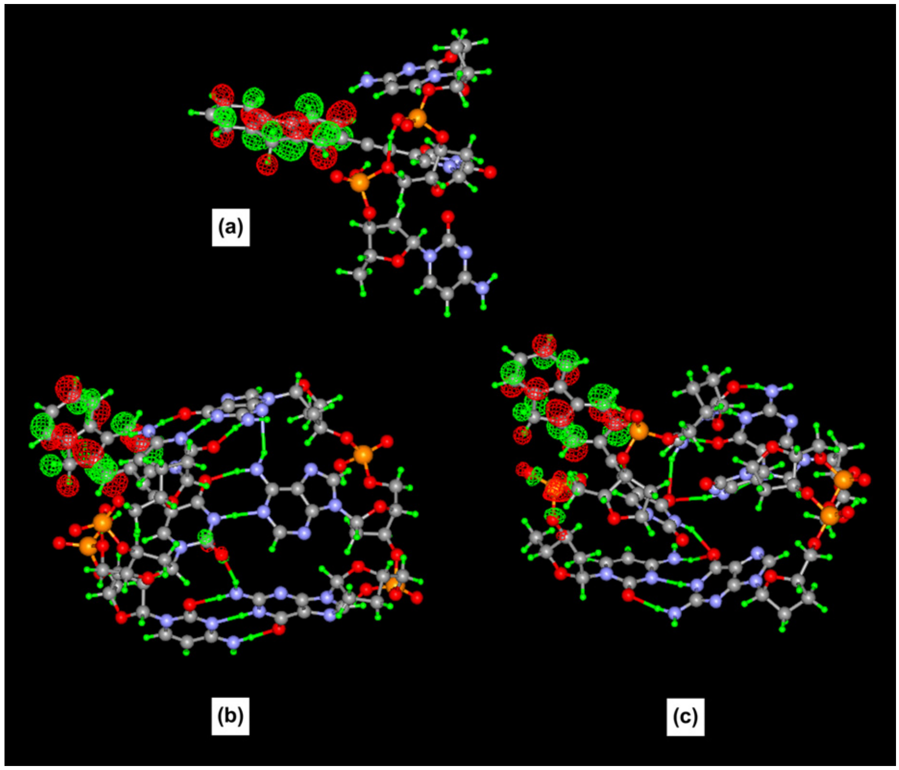

Figure 9. B3LYP/3-21G-predicted structures and unoccupied molecular orbitals of the fluorene units of (a) hairpin ODN2(**U**^{FL}), (b) ODN2(**U**^{FL})/ODN2(**A**), and (c) ODN2(**U**^{FL})/ODN2(**C**).

AM1 calculations.[40] The electronic transitions that had been analyzed from calculations performed using the collective electronic oscillator (CEO) method were recently adapted to explain the fluorescence changes that occur for a fluoride-selective sensor and a fluorescent 'on/off' switch.[41] In addition, the electron–hole interactions occurring under UV irradiation were found to be consistent with a mode of electron transfer occurring between the highest occupied molecular orbital (HOMO) and three lowest unoccupied molecular orbitals (LUMOs).[42] Thus, for large systems where CEO calculations are limited, it seems reasonable to expect that stabilization of the excited molecule would occur when there is an attractive interaction between two regions having accumulated electron densities for the HOMO and LUMOs. Our molecular system is too large to undertake CEO calculations and, thus, we believe that the shapes of the unoccupied molecular orbitals are most critical for understanding the fluorescence properties. Upon excitation at 340 nm, the molecular systems exist in the excited state to give fluorescence at ca. 430 nm. Because this fluorescence originates from the fluorene moiety, the relevant excited state must be related to the unoccupied molecular orbitals of this unit. Unfortunately, in our AM1 calculations the shapes of the unoccupied molecular orbitals look similar in all of the duplexes.

To better understand the experimentally observed fluorescence, we performed ab initio calculations for C**U**^{FL}C, C**U**^{FL}C/GAG, and C**U**^{FL}C/GCG. We selected the A-matched and C-mismatched cases because they provide examples of the purine and pyrimidine series, respectively. We performed all of the calculations at the level of density functional theory (DFT) using the Becke-3-Lee-Yang-Parr (B3LYP) exchange functionals, the Gaussian 98 suite of programs,[43] and 3-21G basis sets. Figure 9 displays the structures and the unoccupied molecular orbitals that are relevant to the occurrence of fluorescence. We note that the hydrogen bonds are not broken in the A-matched case (C**U**^{FL}C/GAG), bearing the anti-conformation, which is different from the situation for the C-mismatched case (C**U**^{FL}C/GCG). We also note that, in the unoccupied molecular orbital of the C-mismatched system, the electron is transferred to a certain extent to the neighboring group, as indicated in Figure 9c. This finding may suggest why there is a dramatic decrease in the fluorescence intensity in the C**U**^{FL}C/GCG system. From our analyses based on the AM1 and ab initio calculations, the fluorescence changes in the hairpin and the matched and mismatched duplexes are caused by both structural rearrangement and charge transfer in the fluorescent excited state. The hydrogen bonds are not broken in the fully matched system (C**U**^{FL}C/GAG) in the ab initio calculations. For the single-base-mismatched duplex (C**U**^{FL}C/GCG), the central uracil unit forms extra hydrogen bonds with its neighboring base unit, but it cannot be paired with the corresponding base units. We expect that this analysis is also valid for the other hairpins ODNs(**U**^{FL}) and their matched and mismatched duplexes [ODNs(**U**^{FL})/ODNs(N), where N=A, T, G, and C].

3. Conclusion

We have synthesized, through Sonogashira coupling, a fluorene-containing deoxyuridine derivative that we incorporated into the loop region of a hairpin. This hairpin functions as new type of MB that requires no fluorescence quencher unit. The fluorescence intensities of single-base-mismatched duplexes are lower than that observed for the hairpin, but they increase upon hybridizing with their fully matched sequences. In particular, the fluorescent ODNs having C-FBs produce efficient fluorescence ON/OFF systems and behave more sensitively as probes than do any other combinations of FBs. These fluorescence differences are extremely dependent on both the triad base pairs, comprising the FBs and the fluorene-modified unit, and the conformation of the $\mathbf{U^{FL}}$/A base pair. From computational calculations, we are convinced that our quencher-free MBs discriminate the mismatched sequences through a diminished emission intensity that occurs through photoinduced charge transfer. There are significant advantages to utilizing this type of MB over more-traditional ones. First, the fluorene-labeled 2′-deoxyuridine unit can be inserted at any position of the oligonucleotide depending on the sequence of interest. Secondly, the 5′ and 3′ ends can be left free to introduce other useful functionalities, e.g., for attachment to surfaces, nanoparticles, or biotin derivatives. Third, our MB synthesis is relatively simple and inexpensive because no quencher is required. Therefore, quencher-free SNP typing using $\mathbf{U^{FL}}$ is a useful and powerful alternative to methods employing conventional SNP typing.

4. Experimental

4.1. Experimental procedures for the synthesis of fluorene-labeled deoxyuridine derivatives

4.1.1. 5′-*O*-[Bis(4-methoxyphenyl)phenylmethyl]-2′-deoxy-5-(2-ethynylfluorenyl)uridine (1). $(PPh_3)_2PdCl_2$ (53 mg, 0.076 mmol) and CuI (14 mg, 0.074 mmol) were added to a solution of 5′-*O*-[bis(4-methoxyphenyl)phenylmethyl]-2′-deoxy-5-iodo uridine (497 mg, 0.757 mmol) and 2-ethynylfluorene (231 mg, 1.21 mmol) in Et_3N (4 mL) and THF (12 mL). Argon was bubbled through the mixture for 2 min before the mixture was subjected 10 times to a pump/purge cycle, and then it was stirred at 45–50 °C for 2 h. After evaporation of solvent in vacuo, the residue was subjected to chromatography (SiO_2; hexane/EtOAc, 1:5) to yield **1** (434 mg, 80%). Recrystallization from $CHCl_3$/MeOH (1:1) gave pure **1**. Mp 160–161 °C. $[\alpha]_D^{14}$ +40 (*c* 1.05, $CHCl_3$). IR (film): ν 3425, 3185, 3013, 2932, 2836, 2261, 1700, 1608, 1508, 1453, 1251, 1177, 1094, 1034, 829, 767, 701, 668 cm^{-1}. ^1H NMR (300 MHz, $CDCl_3$): δ 10.26 (br s, 1H; NH), 8.32 (s, 1H; H-6), 7.73 (d, J=7.4 Hz, 1H; fluorene-H), 7.58–7.51 (m, 4H; fluorene-H), 7.43–7.26 (m, 2H +6H; fluorene-H and DMT-H), 7.15 (d, J=7.5 Hz, 2H; DMT-H), 7.04 (br s, 1H; DMT-H), 6.83 and 6.81 (2d, J=8.5 Hz, 4H; DMT-H), 6.48 (t, J=5.9 Hz, 1H; H-1′), 4.63 (br s, 1H; H-3′), 4.26 (br s, 1H; H-4′), 3.99 (br s, 1H; OH), 3.71 (s, 2H; $ArCH_2$), 3.64 and 3.63 (2s, 6H; OCH_3), 3.50 (br d, J=9.2 Hz, 1H; H-5′), 3.33 (br d, J=8.1 Hz, 1H; H-5′), 2.68 (br s, 1H; H-2′), 2.39 (br s, 1H; H-2′). ^{13}C NMR (75 MHz, $CDCl_3$): δ 162.0, 158.3, 149.6, 144.4, 143.4, 142.5, 142.0, 141.5, 140.9, 135.5, 135.4, 130.2, 129.9, 129.8, 128.1, 127.9, 127.8, 126.9, 126.7, 124.9, 120.3, 120.0, 119.2, 113.2, 100.7, 94.5, 86.8, 85.9, 79.9, 77.2, 72.3, 63.5, 55.0, 41.5, 36.5. HRMS-FAB (*m/z*): $[M+Na]^+$calcd for $C_{45}H_{38}N_2O_7Na$, 741.2578; found, 741.2577.

4.1.2. 5′-*O*-[Bis(4-methoxyphenyl)phenylmethyl]-2′-deoxy-5-(2-ethynylfluorenyl)-3′-[2-cyanoethylbis(1-methylethyl)phosphoramidyl]uridine (2). 2-Cyanoethyldiisopropyl chlorophosphoramidite (120 μL, 0.537 mmol) was added dropwise to a solution of **1** (301 mg, 0. 419 mmol) and 4-formylmorpholine (140 μL, 1.27 mmol) in CH_2Cl_2 (12 mL) at rt. After completion of the reaction (30 min), the mixture was concentrated in vacuo and purified by chromatography through a short column of SiO_2 (hexane/EtOAc, 1:1) to yield **2** (285 mg, 74%). Mp 98–100 °C. $[\alpha]_D^{14}$ +35 (*c* 0.995, $CHCl_3$). IR (film): ν 3186, 3016, 2967, 2837, 2254, 1699, 1608, 1581, 1508, 1455, 1364, 1304, 1251, 1178, 1155, 1035, 880, 830, 771, 667 cm^{-1}. ^1H NMR (300 MHz, $CDCl_3$): δ 8.33 and 8.28 (2s, 1H; NH), 7.74 and 7.71 (2s, 1H; H-6), 7.57–7.48 (m, 4H; fluorene-H), 7.40–7.26 (m, 3H+6H; fluorene-H+DMT-H), 7.17–7.05 (m, 2H; DMT-H), 6.99 and 6.95 (2s, 1H; DMT-H), 6.80 (d, J=8.7 Hz, 4H; DMT-H), 6.39 (dd, J=12.7, 5.6 Hz, 1H; H-1′), 4.63 (br s, 1H; H-3′), 4.26 and 4.21 (2br s, 1H; H-4′), 3.88–3.75 (m, 1H; PCH_2), 3.71 and 3.70 (2s, 2H; $ArCH_2$), 3.67 and 3.65 (2s, 6H; OCH_3), 3.64–3.50 (m, 4H; NCH, PCH_2, H-5′), 3.32–3.28 (m, 1H; H-5′), 2.66–2.58 (m, 2H; CH_2CN, H-2′), 2.46–2.35 (m, 2H; CH_2CN, H-2′), 1.18 and 1.07 (2d, J=6.7 Hz, 12H; $NCHCH_3$). ^{13}C NMR (75 MHz, $CDCl_3$): δ 161.4, 158.5, 149.2, 1443, 144.3, 143.5, 142.5, 141.8, 141.6, 141.0, 135.4, 130.3, 129.9, 128.2, 128.0, 127.0, 126.8, 125.0, 120.4, 120.1, 119.2, 117.6, 117.4, 113.2, 100.8, 94.5, 87.0, 86.2, 85.7, 79.8, 63.2, 63.0, 58.2, 58.0, 55.1, 43.3, 43.2, 43.1, 43.0, 40.8, 36.5, 24.6, 24.5, 20.4, 20.3, 20.2, 20.1, 19.2. ^{31}P NMR (121 MHz, $CDCl_3$): δ 151.6, 151.1. HRMS-FAB (*m/z*): $[M+Na]^+$calcd for $C_{54}H_{55}N_4O_8PNa$, 941.3658; found, 941.3654.

4.2. ODN synthesis and characterization

With a fluorene-labeled deoxyuridine $\mathbf{U^{FL}}$ in hand, we prepared the DMTr-protected 2-cyanoethyl phosphoramidite derivative of $\mathbf{U^{FL}}$ and applied it directly to solid phase oligonucleotide synthesis protocols[23,27] using an automated DNA synthesizer (Perceptive Biosystems 8909 Expedite™ Nucleic Acid Synthesis System). For comparison, the unmodified ODNs were also obtained. The synthesized oligonucleotides were cleaved from the solid support upon treatment with 30% aqueous NH_4OH (1.0 mL) for 10 h at 55 °C. The crude products from the automated ODN synthesis were lyophilized and diluted with distilled water (1 mL). The ODNs were purified using HPLC (Merck LichoCART C18 column, 10×250 mm, 10 μm, 100 Å pore size). The HPLC mobile phase was held isocratically for 10 min using 5% acetonitrile/0.1 M triethylammonium acetate (TEAA; pH 7.0) at a flow rate of 2.5 mL/min. The gradient was then increased linearly over 10 min from 5% acetonitrile/0.1 M TEAA to 50% acetonitrile/0.1 M TEAA at the same flow rate. The fractions containing the purified ODN were pooled and lyophilized. Aqueous AcOH (80%) was added to the ODN. After standing for 30 min at ambient temperature, the AcOH was evaporated under reduced pressure. The residue was diluted with water (1 mL) and then the solution was purified using HPLC under the same conditions as described above. The ODNs were analyzed using HPLC

(Hewlett–Packard, ODS Hypersil, 4.6×200 mm, 5 μm, 79916OD-574) and almost the same eluent system, but at a different flow rate (1 mL/min). For characterization, matrix-assisted laser desorption ionization time-of-flight (MALDI-TOF) mass spectrometric data of the $\mathbf{U^{FL}}$ oligonucleotides were collected using a PE Biosystems Voyager System 4095 operated in the positive-ion mode and using a 1:1 mixture of 3-hydroxypicolinic acid (0.35 M) and ammonium citrate (0.1 M) as the matrix; the accelerating voltage was 25 kV.

4.3. Melting temperature (T_m) measurements

All values of T_m of the ODNs (1.5 μM) were recorded in 100 mM Tris–HCl buffers (pH 8.0) containing 1 mM $MgCl_2$. Absorbance versus temperature profiles were measured at 260 nm using a Cary 100 Conc UV–vis spectrophotometer (Varian) equipped with a temperature controller and using a 1 cm path length cell. The absorbance of the samples was monitored at 260 nm over the temperature range from 6 to 90 °C using a heating rate of 1 °C/min. From these profiles, first derivatives were calculated to determine the values of T_m.

4.4. UV absorption measurements

ODN solutions were prepared as described above for the T_m measurements. Absorption spectra were obtained using a Cary 100 Conc UV–vis spectrophotometer at room temperature and using a 1 cm path length cell.

4.5. Circular dichroism (CD) spectroscopy

The mixture of ODNs was equilibrated by cooling to 5 °C; after 30 min the CD spectra were recorded using a Jasco J-715 CD spectropolarimeter. The temperature was controlled using a Jasco PTC-348WI temperature controller.

4.6. Fluorescence experiments

ODN solutions were prepared as described above for the T_m measurements. Fluorescence spectra were obtained at 37 °C using a PTI Fluorescence System spectrofluorophotometer and a 1 cm path length cell. The excitation bandwidth was 1 nm. The emission bandwidth was 1 nm. The fluorescence quantum yields (Φ_F) were determined using 9,10-diphenylanthracene as a reference; it has a known value of Φ_F in ethanol of 0.95. The area of the emission spectrum was integrated using the software available in the instrument, and the quantum yield was calculated according to the following equation:

$$\Phi_{F(S)}/\Phi_{F(R)} = \left[A_{(S)}/A_{(R)}\right] \times \left[(\mathrm{Abs})_{(R)}/(\mathrm{Abs})_{(S)}\right] \times \left[n^2_{(S)}/n^2_{(R)}\right]$$

Here, $\Phi_{F(S)}$ and $\Phi_{F(R)}$ are the fluorescence quantum yields of the sample and reference, respectively; $A_{(S)}$ and $A_{(R)}$ are the areas under the fluorescence spectra of the sample and the reference, respectively; $(\mathrm{Abs})_{(S)}$ and $(\mathrm{Abs})_{(R)}$ are the respective optical densities of the sample and the reference solution at the wavelength of excitation; $n_{(S)}$ and $n_{(R)}$ are the values of refractive index for the respective solvents used to prepare the sample and the reference.

Acknowledgements

We thank KOSEF for their financial support through the National Research Laboratory Program (Laboratory for Modified Nucleic Acid Systems), Gene Therapy R&D Program (M10534000011-05N3400-01110), and KNRRC Program.

Supplementary data

The supplementary information has MALDI-TOF mass spectral data, photophysical properties of the matched and mismatched fluorene-labeled ODN($\mathbf{U^{FL}}$)duplexes, and excitation spectra of the ssDNA and dsDNA. Supplementary data associated with this article can be found in the online version, at doi:10.1016/j.tet.2006.10.091.

References and notes

1. (a) Licinio, L.; Wong, M. *Pharmacogenomics*; Wiley-VCH: Weinheim, 2002; (b) McCarthy, J. J.; Hilfiker, R. *Nat. Biotechnol.* **2000**, *18*, 505; (c) Stoneking, M. *Nature* **2001**, *409*, 821; (d) Chakravarti, A. *Nature* **2001**, *409*, 928; (e) Evans, W. E.; Relling, M. V. *Science* **1999**, *286*, 487.
2. (a) www.ncbi.nlm.nih.gov/disease; (b) Relling, M. V.; Dervieux, T. *Nat. Rev. Cancer* **2001**, *1*, 99.
3. (a) Nakatani, K. *Chembiochem* **2004**, *5*, 1623; (b) Ho, H. A.; Boissinot, M.; Bergeron, M. G.; Corbeil, G.; Dore, K.; Boudreau, D.; Leclerc, M. *Angew. Chem., Int. Ed.* **2002**, *41*, 1548; (c) Tyagi, S.; Kramer, F. R. *Nat. Biotechnol.* **1996**, *14*, 303.
4. Ho, H. A.; Boissinot, M.; Bergeron, M. G.; Corbeil, G.; Dore, K.; Boudreau, D.; Leclerc, M. *Angew. Chem., Int. Ed.* **2002**, *41*, 1548.
5. (a) Olivier, M.; Chuang, L. M.; Chang, M. S.; Chen, Y. T.; Pei, D.; Ranade, K.; de Witte, A.; Allen, J.; Tran, N.; Curb, D.; Pratt, R.; Neefs, H.; Indig, M. D.; Law, S.; Neri, B.; Wang, L.; Cox, D. R. *Nucleic Acids Res.* **2002**, *30*, e53; (b) Lyamichev, V.; Mast, A. L.; Hall, J. G.; Prudent, J. R.; Kaiser, M. W.; Takova, T.; Kwiatkowski, R. W.; Sander, T. J.; de Arruda, M.; Arco, D. A.; Neri, B. P.; Brow, M. A. D. *Nat. Biotechnol.* **1999**, *17*, 292.
6. Komiyama, M.; Ye, S.; Liang, X. G.; Yamamoto, Y.; Tomita, T.; Zhou, J. M.; Aburatani, H. *J. Am. Chem. Soc.* **2003**, *125*, 3758.
7. (a) Syvanen, A. C. *Hum. Mutat.* **1999**, *13*, 1; (b) Pastinen, T.; Kurg, A.; Metspalu, A.; Peltonen, L.; Syvanen, A. C. *Genome Res.* **1997**, *7*, 606.
8. Pastinen, T.; Raitio, M.; Lindroos, K.; Tainola, P.; Peltonen, L.; Syvanen, A. C. *Genome Res.* **2000**, *10*, 1031.
9. (a) Schena, M.; Heller, R. A.; Theriault, T. P.; Konrad, K.; Lachenmeier, E.; Davis, R. W. *Trends Biotechnol.* **1998**, *16*, 301; (b) Pirrung, M. C. *Angew. Chem., Int. Ed.* **2002**, *41*, 1276.
10. (a) Taton, T. A.; Mirkin, C. A.; Letsinger, R. L. *Science* **2000**, *289*, 1757; (b) Liu, G.; Lee, T. M. H.; Wang, J. *J. Am. Chem. Soc.* **2005**, *127*, 38.
11. (a) Morrison, L. E. *J. Fluoresc.* **1999**, *9*, 187; (b) Didenko, V. V. *Biotechniques* **2001**, *31*, 1106; (c) Foy, C. A.; Parkes, H. C. *Clin. Chem.* **2001**, *47*, 990; (d) Kricka, L. J. *Ann. Clin. Biochem.* **2002**, *39*, 114.
12. Joshi, H. S.; Tor, Y. *Chem. Commun.* **2001**, 549.

13. Zhang, P.; Beck, T.; Tan, W. *Angew. Chem., Int. Ed.* **2001**, *40*, 402.
14. Ranasinghe, R. T.; Brown, L. J.; Brown, T. *Chem. Commun.* **2001**, 1480.
15. Dobson, N.; McDowell, D. G.; French, D. J.; Brown, L. J.; Mellor, J. M.; Brown, T. *Chem. Commun.* **2003**, 1234.
16. Stojanovic, M. N.; de Prada, P.; Landry, D. W. *Chembiochem* **2001**, *2*, 411.
17. Fujimoto, K.; Shimizu, H.; Inouye, M. *J. Org. Chem.* **2004**, *69*, 3271.
18. Hawkins, M. E.; Bails, F. M. *Nucleic Acids Res.* **2004**, *32*, e62.
19. (a) Rist, M. J.; Marino, J. P. *Curr. Org. Chem.* **2002**, *6*, 775; (b) Daniels, M.; Hauswirth, W. *Science* **1971**, *171*, 675; (c) Pecourt, J. M. L.; Peon, J.; Kohler, B. *J. Am. Chem. Soc.* **2000**, *122*, 9348; (d) Jean, J. M.; Hall, K. B. *Proc. Natl. Acad. Sci. U.S.A.* **2001**, *98*, 37; (e) Singleton, S. F.; Shan, F.; Kanan, M. W.; McIntosh, C. M.; Stearman, C. J.; Helm, J. S.; Webb, K. J. *Org. Lett.* **2001**, *3*, 3919; (f) Okamoto, A.; Tanaka, T.; Fukuda, T.; Saito, I. *J. Am. Chem. Soc.* **2003**, *125*, 9296.
20. (a) Secrist, J. A., III; Barrio, J. R.; Leonard, N. J. *Science* **1972**, *175*, 646; (b) Holmen, A.; Albinsson, B.; Norden, B. *J. Phys. Chem.* **1994**, *98*, 13460.
21. (a) Hwang, G. T.; Seo, Y. J.; Kim, B. H. *J. Am. Chem. Soc.* **2004**, *126*, 6528; (b) Seo, Y. J.; Ryu, J. H.; Kim, B. H. *Org. Lett.* **2005**, *7*, 4931; (c) Venkatesan, N.; Seo, Y. J.; Bang, E. K.; Park, S. M.; Lee, Y. S.; Kim, B. H. *Bull. Korean Chem. Soc.* **2006**, *27*, 613.
22. (a) Hurley, D. J.; Tor, Y. *J. Am. Chem. Soc.* **2002**, *124*, 3749; (b) Kottysch, T.; Ahlborn, C.; Brotzel, F.; Richert, C. *Chem.—Eur. J.* **2004**, *10*, 4017.
23. Modified oligonucleotides were synthesized as described previously using standard solid phase phosphoramidite chemistry. See: Kim, S. J.; Kim, B. H. *Nucleic Acids Res.* **2003**, *31*, 2725.
24. Sheardy, R. D.; Seeman, N. C. *J. Org. Chem.* **1986**, *51*, 4301.
25. Tani, H.; Toda, F.; Matsumiya, K. *Bull. Chem. Soc. Jpn.* **1963**, *36*, 391.
26. (a) Sonogashira, K. *Metal-Catalyzed Cross-Coupling Reactions*; Diederich, F., Stang, P. J., Eds.; Wiley-VCH: Weinheim, 1998; (b) Sonogashira, K.; Tohda, Y.; Hagihara, N. *Tetrahedron Lett.* **1975**, 4467; (c) Hwang, G. T.; Son, H. S.; Ku, J. K.; Kim, B. H. *Org. Lett.* **2001**, *3*, 2469; (d) Hwang, G. T.; Son, H. S.; Ku, J. K.; Kim, B. H. *J. Am. Chem. Soc.* **2003**, *125*, 11241; (e) Hwang, G. T.; Seo, Y. J.; Kim, S. J.; Kim, B. H. *Tetrahedron Lett.* **2004**, *45*, 3543; (f) Hwang, G. T.; Kim, B. H. *Org. Lett.* **2004**, *6*, 2669; (g) Seo, Y. J.; Ryu, J. H.; Kim, B. H. *Org. Lett.* **2005**, *7*, 4931; (h) Seo, Y. J.; Kim, B. H. *Chem. Commun.* **2006**, 150.
27. Gait, M. J. *Oligonucleotide Synthesis: A Practical Approach*; IRL: Washington, DC, 1984.
28. (a) Amann, N.; Pandurski, E.; Fiebig, T.; Wagenknecht, H.-A. *Chem.—Eur. J.* **2002**, *8*, 4877; (b) Raytchev, M.; Mayer, E.; Amann, N.; Wagenknecht, H.-A.; Fiebig, T. *Chemphyschem* **2004**, *5*, 706.
29. (a) Steenken, S.; Telo, J. P.; Novais, H. M.; Candeias, L. P. *J. Am. Chem. Soc.* **1992**, *114*, 4701; (b) Seidel, C. A. M.; Schulz, A.; Sauer, M. H. M. *J. Phys. Chem.* **1996**, *100*, 5541; (c) Voityuk, A. A.; Michel-Beyerle, M.-E.; Rösch, N. *Chem. Phys. Lett.* **2001**, *342*, 231; (d) Wagenknecht, H.-A. *Angew. Chem., Int. Ed.* **2003**, *42*, 2454.
30. (a) O'Connor, D.; Shafirovich, V. Y.; Geacintov, N. E. *J. Phys. Chem.* **1994**, *98*, 9831; (b) Shafirovich, V. Y.; Courtney, S. H.; Ys, N.; Geacintov, N. E. *J. Am. Chem. Soc.* **1995**, *117*, 4920; (c) Lewis, F. D.; Letsinger, R. L.; Wasielewski, M. R. *Acc. Chem. Res.* **2001**, *34*, 159; (d) Heinlein, T.; Knemeyer, J.-P.; Piestert, O.; Sauer, M. *J. Phys. Chem. B* **2003**, *107*, 7957; (e) Crockett, A. O.; Wittwer, C. T. *Anal. Biochem.* **2001**, *290*, 89.
31. (a) Okamoto, A.; Kanatani, K.; Saito, I. *J. Am. Chem. Soc.* **2004**, *126*, 4820; (b) Hwang, G. T.; Seo, Y. J.; Kim, B. H. *Tetrahedron Lett.* **2005**, *46*, 1475.
32. Koenig, P.; Reines, S. A.; Cantor, C. R. *Biopolymers* **1977**, *16*, 2231.
33. (a) Nakatani, K.; Okamoto, A.; Matsuno, T.; Saito, I. *J. Am. Chem. Soc.* **1998**, *120*, 11219; (b) Nakatani, K.; Sando, S.; Saito, I. *Nat. Biotechnol.* **2001**, *19*, 51.
34. (a) Ito, T.; Rokita, S. E. *J. Am. Chem. Soc.* **2004**, *126*, 15552; (b) Acharya, S.; Barman, J.; Cheruku, P.; Chatterjee, S.; Acharya, P.; Isaksson, J.; Chattopadhyaya, J. *J. Am. Chem. Soc.* **2004**, *126*, 8674.
35. (a) Yoshimoto, K.; Nishizawa, S.; Minagawa, M.; Teramae, N. *J. Am. Chem. Soc.* **2003**, *125*, 8982; (b) Matray, T. J.; Kool, E. T. *J. Am. Chem. Soc.* **1998**, *120*, 6191.
36. Demole, B.; Harrison, L. *Annu. Rev. Biochem.* **1994**, *63*, 915.
37. (a) Nakatani, K.; Sando, S.; Saito, I. *J. Am. Chem. Soc.* **2000**, *122*, 2172; (b) Nakatani, K.; Horie, S.; Saito, I. *J. Am. Chem. Soc.* **2003**, *125*, 8972.
38. For examples, see: (a) Kaden, P.; Mayer-Enthart, E.; Trifonov, A.; Fiebig, T.; Wagenknecht, H.-A. *Angew. Chem., Int. Ed.* **2005**, *44*, 1636; (b) Refs. 31a and 35a.
39. (a) Kabelac, M.; Zendlova, L.; Reha, D.; Hobza, P. *J. Phys. Chem. B* **2005**, *109*, 12206; (b) Kawahara, S.-i.; Uchimaru, T.; Taira, K.; Sekine, M. *J. Phys. Chem. A* **2002**, *106*, 3207; (c) Blancafort, L.; Bertran, J.; Sodupe, M. *J. Am. Chem. Soc.* **2004**, *126*, 12770; (d) Asensio, A.; Kobko, N.; Dannenberg, J. J. *J. Phys. Chem. A* **2003**, *107*, 6441.
40. Dewar, M. J. S.; Zoebisch, E. G.; Healy, E. F.; Stewart, J. J. P. *J. Am. Chem. Soc.* **1985**, *107*, 3902.
41. (a) Cho, E. J.; Moon, J. W.; Ko, S. W.; Lee, J. Y.; Kim, S. K.; Yoon, J.; Nam, K. C. *J. Am. Chem. Soc.* **2003**, *125*, 12376; (b) Lee, J. Y.; Cho, E. J.; Mukamel, S.; Nam, K. C. *J. Org. Chem.* **2004**, *69*, 943.
42. Kim, S. K.; Lee, S. H.; Lee, J. Y.; Lee, J. Y.; Bartsch, R. A.; Kim, J. S. *J. Am. Chem. Soc.* **2004**, *126*, 16499.
43. Frisch, M. J.; Trucks, G. W.; Schlegel, H. B.; Scuseria, G. E.; Robb, M. A.; Cheeseman, J. R.; Zakrzewski, V. G.; Montgomery, J. A.; Stratmann, R. E.; Burant, J. C.; Dapprich, S.; Millam, J. M.; Daniels, A. D.; Kudin, K. N.; Strain, M. C.; Farkas, O.; Tomasi, J.; Barone, V.; Cossi, M.; Cammi, R.; Mennucci, B.; Pomelli, C.; Adamo, C.; Clifford, S.; Ochterski, J.; Petersson, G. A.; Ayala, P. Y.; Cui, Q.; Morokuma, K.; Malick, D. K.; Rabuck, A. D.; Raghavachari, K.; Foresman, J. B.; Cioslowski, J.; Ortiz, J. V.; Baboul, A. G.; Stefanov, B. B.; Liu, G.; Liashenko, A.; Piskorz, P.; Komaromi, I.; Gomperts, R.; Martin, R. L.; Fox, D. J.; Keith, T.; AlLaham, M. A.; Peng, C. Y.; Nanayakkara, A.; Gonzalez, C.; Challacombe, M.; Gill, P. M. W.; Johnson, B.; Chen, W.; Wong, M. W.; Andres, J. L.; Gonzalez, C.; Head-Gordon, M.; Replogle, E. S.; Pople, J. A. *Gaussian 98, revision A.6*; Gaussian: Pittsburgh, PA, 1998.